Biochimica et Biophysica Acta, 1019 (1990) 29–41
Elsevier

BBABIO 43246

Genetic analysis of a 9 kDa phycocyanin-associated linker polypeptide

Robert de Lorimier *, Donald A. Bryant and S. Edward Stevens, Jr. **

Department of Molecular and Cell Biology, The Pennsylvania State University, University Park, PA (U.S.A.)

(Received 7 August 1989)
(Revised manuscript received 2 April 1990)

Key words: Phycobilisome; Linker polypeptide; Phycocyanin; Directed mutation; (*Synechococcus* sp. PCC 7002); (*A. quadruplicatum*)

The gene encoding LR9, a 9 kDa phycocyanin-associated linker polypeptide, was cloned from the cyanobacterium *Synechococcus* sp. PCC 7002 (*Agmenellum quadruplicatum* PR-6). This gene, termed *cpcD*, was located immediately 3′ to *cpcC*, a gene which encodes another phycocyanin-associated linker, LR33. Mutation of *cpcD* by insertion led to the loss of LR9 as the only detectable change in phycobilisome composition. Cells and isolated phycobilisomes from the *cpcD*⁻ strain did not detectably differ from the wild-type in absorption or steady-state fluorescence emission. Purified phycobilisomes from the wild-type and *cpcD*⁻ strains were compared by electron microscopy. The number of phycocyanin discs in the rod substructures of the mutant was more variable than in the wild-type. Hence, one function of LR9 may be to minimize the heterogeneity of rod length, possibly by binding to the core-distal face of phycocyanin-LR33 complexes to prevent the tandem joining of such units. A mutant in which *cpcD* and *cpcC-cpcD* intergenic sequences are deleted shows a partial loss of LR33. Inverted repeats in this intergenic region may be required for optimal stability of the *cpcC* transcript.

Introduction

We are analyzing the structure, function and regulation of phycobilisomes by a molecular genetic approach. The subject organism for much of this work has been *Synechococcus* sp. PCC 7002 (*Agmenellum quadruplicatum* PR-6), a unicellular cyanobacterium that is genetically transformable [1]. Its phycobilisomes are relatively simple and are comprised of eleven different polypeptides [2]. The genes *cpcA* and *cpcB*, encoding the α and β subunits of phycocyanin (PC), respectively have been cloned [3]. These genes are single-copy and linked in tandem, with *cpcB* located 5′ to *cpcA*. Subsequently, a phycobilisome gene which encodes a 33 kDa PC-associated linker polypeptide, termed LR33, was found immediately 3′ to *cpcA* [4,5]. Mutation of this gene, called *cpcC*, confirmed one function of the polypeptide, that of linking PC hexamers in tandem to form rod substructures.

In a search for yet other phycobilisome genes we cloned and sequenced a segment of the genome located 3′ to *cpcC*. As a result, three genes related to the organization and synthesis of PC were found. This report concerns the gene immediately 3′ to *cpcC*, called *cpcD*, which is shown to encode another PC-associated linker polypeptide. Also described are the consequences of mutating *cpcD*. We have previously outlined some of these results, including the deduced amino-acid sequence of the linker encoded by *cpcD* [5].

The sequence data in this paper have been submitted to the EMBL/Genbank Data Libraries.

Present addresses:
* Department of Molecular and Cell Biology, Stanley/Donner ASU, University of California, Berkeley, CA, U.S.A.
** Department of Biological Sciences, Memphis State University, Memphis, TN, U.S.A.

Abbreviations: AP, allophycocyanin; PC, phycocyanin; PEC, phycoerythrocyanin. Linker polypeptides are abbreviated according to the nomenclature proposed by A.N. Glazer [18], but subscripts and superscripts are placed on the line of type. L(X)(Y) refers to a linker polypeptide located at a position (X), where (X) is R (rod), C (core), RC (rod-to-core) or CM (core-to-membrane), and which has an apparent molecular mass of (Y) kDa. When it is necessary to distinguish the class of phycobiliprotein to which a rod linker is bound, the abbreviation of that class is appended to the name of the linker; for example, LR34.5PEC is a rod linker of 34.5 kDa that is associated with phycoerythrocyanin.

Correspondence: D.A. Bryant, Department of Molecular and Cell Biology, The Pennsylvania State University, University Park, PA 16802, U.S.A.

Materials and Methods

Cloning and nucleotide sequence of cpcD

A *Pst*I digest of *Synechococcus* sp. PCC 7002 total DNA was fractionated by electrophoresis in a 0.5% agarose gel. DNA fragments in the range of 4.5 to 6.5 kb were eluted from the gel and ligated with pUC8 [6] that had been digested with *Pst*I and treated with alkaline phosphatase. Ligated DNA was transformed into *Escherichia coli* strain RDP145 [7]. Ampicillin-resistant colonies were probed for homology to *cpcC*, by using the 0.5 kb *Xho*I/*Hpa*I fragment of pAQPR1 [3] (see Fig. 1) according to the colony hybridization method of Hanahan and Meselson [8]. Positive isolates all contained plasmid DNA with inserts having the structure shown on the top line of Fig. 1. This plasmid was called pAQPR50. The nucleotide sequence of its 358 bp *Hin*dIII fragment was determined by the chain termination method [9] using synthetic oligonucleotide primers based on sequences flanking the fragment.

Construction of strains mutated in cpcD

(A) Strain PR6011. The 3.2 kb *Xho*I fragment of pAQPR50 was subcloned into the *Sal*I site of pUC7 [6], generating pAQPR52. This plasmid was digested with *Hin*dIII and treated with the large fragment of *E. coli* DNA polymerase I to fill in the ends. Ligated to this DNA was the 1.3 kb *Hin*dIII/*Sma*I fragment of pAQE17 [10], which carries the aminoglycoside 3′-phosphotransferase II (*aph*) gene of Tn5. This fragment had also been treated to fill in its *Hin*dIII end. Ligated DNA was transformed into *E. coli* under selection for resistance to kanamycin. Plasmid pAQPR56 (Fig. 1) was found by screening drug-resistant isolates. This plasmid was transformed into *Synechococcus* sp. PCC 7002 as previously described [7]. Prior to transformation the DNA was rendered linear by digesting with *Bam*HI, the purpose of which was to prevent integration of the entire plasmid into the cyanobacterial genome. Cyanobacterial isolates resistant to kanamycin at 150 μg/ml arose at a frequency of approx. 10^{-1} per colony-forming unit. One isolate was streak-purified and called PR6011.

(B) Strain PR6014. The coding region of *cpcD* lacks restriction sites suitable for constructing an insertion mutation. Instead, we produced a mutation in which part of the coding region was deleted and replaced with the kanamycin-resistance gene. First, exonuclease III and nuclease S1 [11] were used to generate unidirectional deletions at either end of the 358 bp *Hin*dIII fragment. An octanucleotide *Sma*I linker (New England BioLabs) was ligated to the deleted ends. Clones of the *Hin*dIII fragment deleted of its 3′ half were fused with clones deleted of its 5′ half. This was accomplished by ligation of the clones after digesting with *Ava*I, which cuts only at the *Sma*I linker attached to the deletion endpoints. One particular fusion was sequenced and found to contain the 5′ 168 bp (nucleotides 119 to 286 in Fig. 2) of the original fragment joined to the 3′ 125 bp (nucleotides 352 to 476). This clone therefore contains all of the original *Hin*dIII fragment except for 65 bp in the center of *cpcD* (Fig. 2). A marker gene, the same *aph* gene fragment as used for the construction of *cpcD*1, was inserted at the *Sma*I site. A clone which had the *aph* gene oriented in the same transcriptional polarity as *cpcD* was isolated. DNA of this clone failed to transform *Synechococcus* sp. PCC 7002 to kanamycin resistance, probably because of insufficient lengths of homology, 168 and 125 bp, to the cyanobacterial genome. Therefore, the interrupted *cpcD* gene of this clone, as a 1.6 kb *Hin*dIII fragment, was cloned into pAQPR52 (see above) to replace the 358 bp *Hin*dIII fragment of the latter. This resulted in plasmid pAQPR56-2 (Fig. 1), which was transformed into *Synechococcus* sp. PCC 7002 without prior linearization. Kanamycin-resistant transformants, one of which was isolated and called PR6014, arose at a frequency of about 10^{-1} per colony-forming unit. This strain and PR6011 were routinely grown in medium containing kanamycin at 50 μg/ml. Antibiotic was omitted when the growth rates of these strains were being compared to that of the wild-type.

Phycobilisome isolation

Synechococcus sp. PCC 7002 was grown in medium A [12] containing $NaNO_3$ at 1 g/l. Cells were kept in suspension by mixing with a magnetic stirring bar. The medium was maintained at 32° C, bubbled continuously with 1% CO_2 in air, and illuminated with cool white fluorescent lamps at an intensity of 200 $\mu E/m^2$ per s. Phycobilisomes were purified as previously described [4]. Absorption spectra were determined on a Cary 14 double-beam spectrophotometer modified for computerized data acquisition. Fluorescence emission spectra were obtained with Perkin Elmer MPF66 or SLM Aminco 8000C spectrofluorometers. The excitation and emission bandwidths were 4 nm. Fluorescence intensity was measured ratiometrically with Rhodamine B as a quantum counter.

Electron microscopy

The procedure of Yamanaka et al. [13] was followed with minor alterations. Freshly isolated phycobilisomes in 0.75 M sucrose/0.75 M $KHPO_4$ (pH 7.0)/2 mM Na_2EDTA/2 mM NaN_3 were diluted 20-fold in a drop of the same buffer to a phycobiliprotein concentration of 50 μg/ml. A formvar-coated grid was immediately placed on the drop for 30 s, whereupon it was removed, blotted dry and placed on a drop of the same buffer containing 3% (w/v) glutaraldehyde. After 5 min the grid was blotted dry and transferred sequentially to drops of the original diluent, 100 mM ammonium

acetate, 10 mM ammonium acetate, and 1% uranyl acetate, blotting the grid carefully between each. Grids were held for 60 s on the stain and 30 s on other solutions.

Micrographs were obtained on a Philips EM 300 electron microscope at a primary magnification of 40 000 ×. Particles which had the characteristic core structure, i.e., three triangularly arranged circular objects, and at least four rod substructures were scored as phycobilisomes. Phycobilisome-like particles with less than four rods were very rare. A sample of 108 phycobilisomes was evaluated from strains PR6000 and PR6014 each. For each phycobilisome the number of rods and number of discs on each rod were recorded. From these data we obtained for each strain a distribution of the number of rods per phycobilisome, the number of discs per rod and the number of discs per phycobilisome. To compare the strains in terms of these parameters we employed the *t* statistic to test differences between means, the *F* distribution to test differences in variance, and the chi-square statistic to test differences in proportion and goodness-of-fit. A value of *P* (the probability of rejecting a true hypothesis) less than or equal to 0.05 was considered significant.

Results

Molecular cloning and nucleotide sequence of cpcD

In previous work we had cloned a 3.0 kb *Hin*dIII fragment of the *Synechococcus* sp. PCC 7002 (*Agmenellum quadruplicatum* strain PR-6) genome which carries three tandem genes, *cpcBAC*, encoding βPC, αPC, and LR33, respectively [3,4] (Fig. 1). To determine whether additional genes related to the phycobilisome were encoded 3′ to *cpcC*, we sought to clone genomic sequences extending beyond this gene. Southern blots of genomic DNA probed with subclones of the 3.0 kb *Hin*dIII fragment showed that a 6.1 kb *Pst*I fragment would contain *cpcAC*, together with 4.4 kb of 3′ sequences. This particular *Pst*I fragment was cloned as pAQPR50 (Materials and Methods). Restriction map data from pAQPR1 and pAQPR50 are combined in Fig. 1 to show the structure of a 7.4 kb segment of the genome which includes *cpcBAC*.

The nucleotide sequence of the 358 bp *Hin*dIII fragment immediately 3′ to *cpcC* was determined (Materials and Methods) and is displayed in Fig. 2. The longest open reading frame contained in this fragment is also shown in Fig. 2, and is translated into an amino-acid sequence. The putative product of the open reading frame is composed of 80 amino acid residues, is initiated at a methionine residue, terminates at a UAA codon, and has a putative Shine-Dalgarno sequence close to the initiation site (Fig. 2). The predicted molecular mass of the product is 9055 Da. We had demonstrated the presence of a 9 kDa polypeptide, termed LR9, associated with PC from purified phycobilisomes [4]. Because of this similarity in mass, the proximity of this open reading frame to other rod-related genes, and partial amino-acid sequence homology between LR33 and the encoded polypeptide (see Discussion), we hypothesized that the open reading frame encoded LR9.

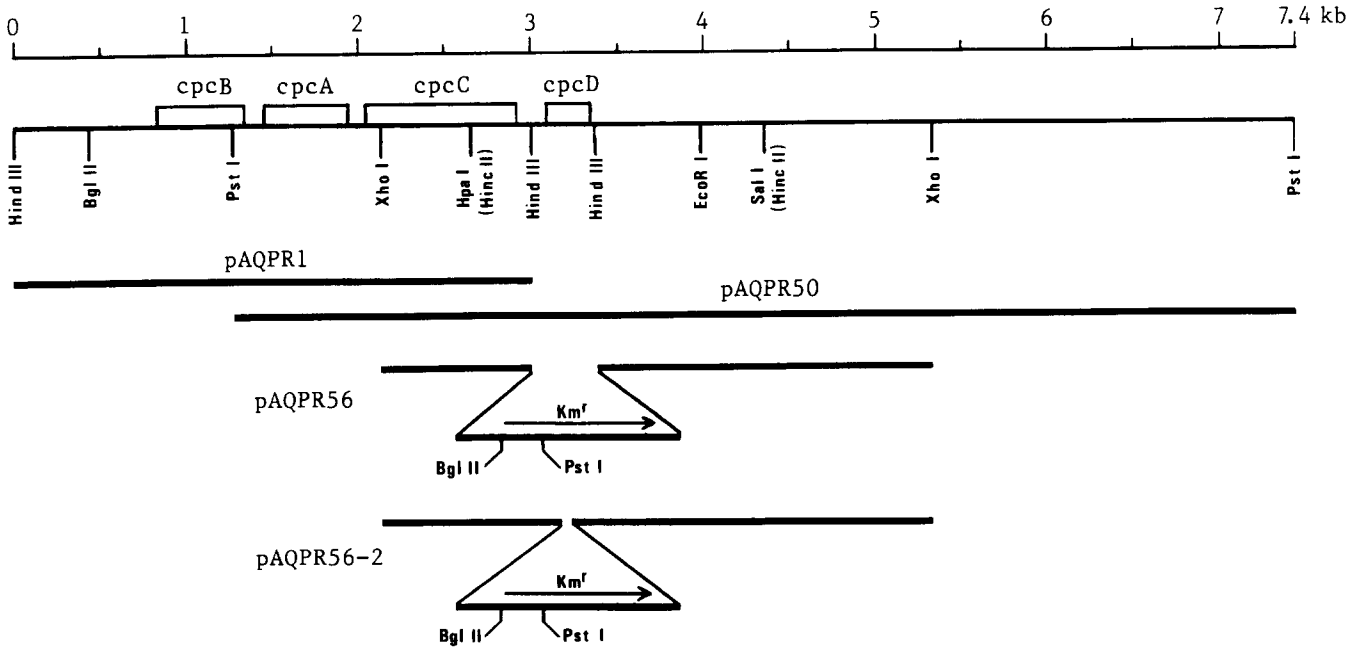

Fig. 1. Restriction maps of cloned *Synechococcus* sp. PCC 7002 genomic DNA fragments containing genes of the phycocyanin-encoding locus (pAQPR1 and pAQPR50). Also delineated are two derivatives of the 3.2 kb *Xho*I fragment which are totally or partially deleted of *cpcD* and contain a corresponding insertion of the *aph* (Km^r) fragment of Tn5 (pAQPR56 and pAQPR56-2).

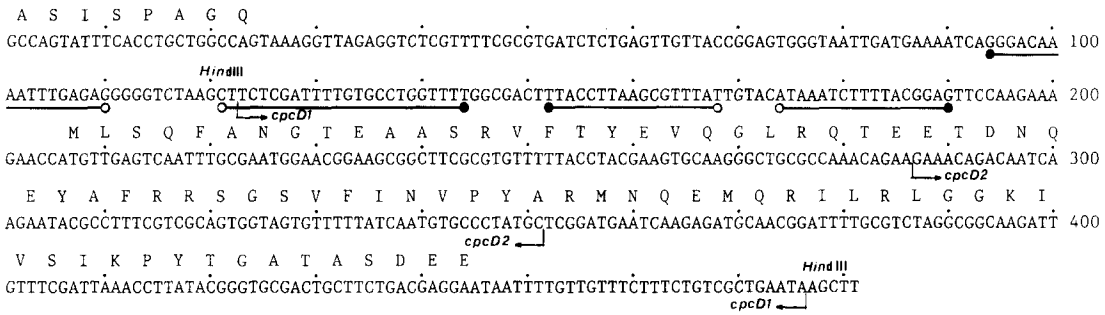

Fig. 2. Nucleotide sequence of the 358 bp *Hin*dIII fragment containing *cpcD*. The fragment extends from nucleotides 118 to 476, as numbered. Also shown are 120 bp of contiguous sequence located 5′ to the *Hin*dIII fragment which include the 3′ terminus of *cpcC* and the intercistronic region. A deduced amino-acid sequence for LR9 is shown above the *cpcD* coding region (nucleotides 207 to 448), and the carboxyl terminal 8 residues of LR33 are shown above the 3′-terminal coding region of *cpcC* (nucleotides 1–27). Nucleotides missing in the *cpcD*1 deletion (113–476) and *cpcD*2 deletion (287–351) are indicated. Also delineated are two inverted repeats located in the intercistronic region. One extends from nucleotide 94 to 144, the other from nucleotide 152 to 190. The underlined segments of each could, in a transcript, form the stem of a stem-loop structure. Paired nucleotides at the base of the stem are shown as solid dots, while those at the loop end are shown as open circles.

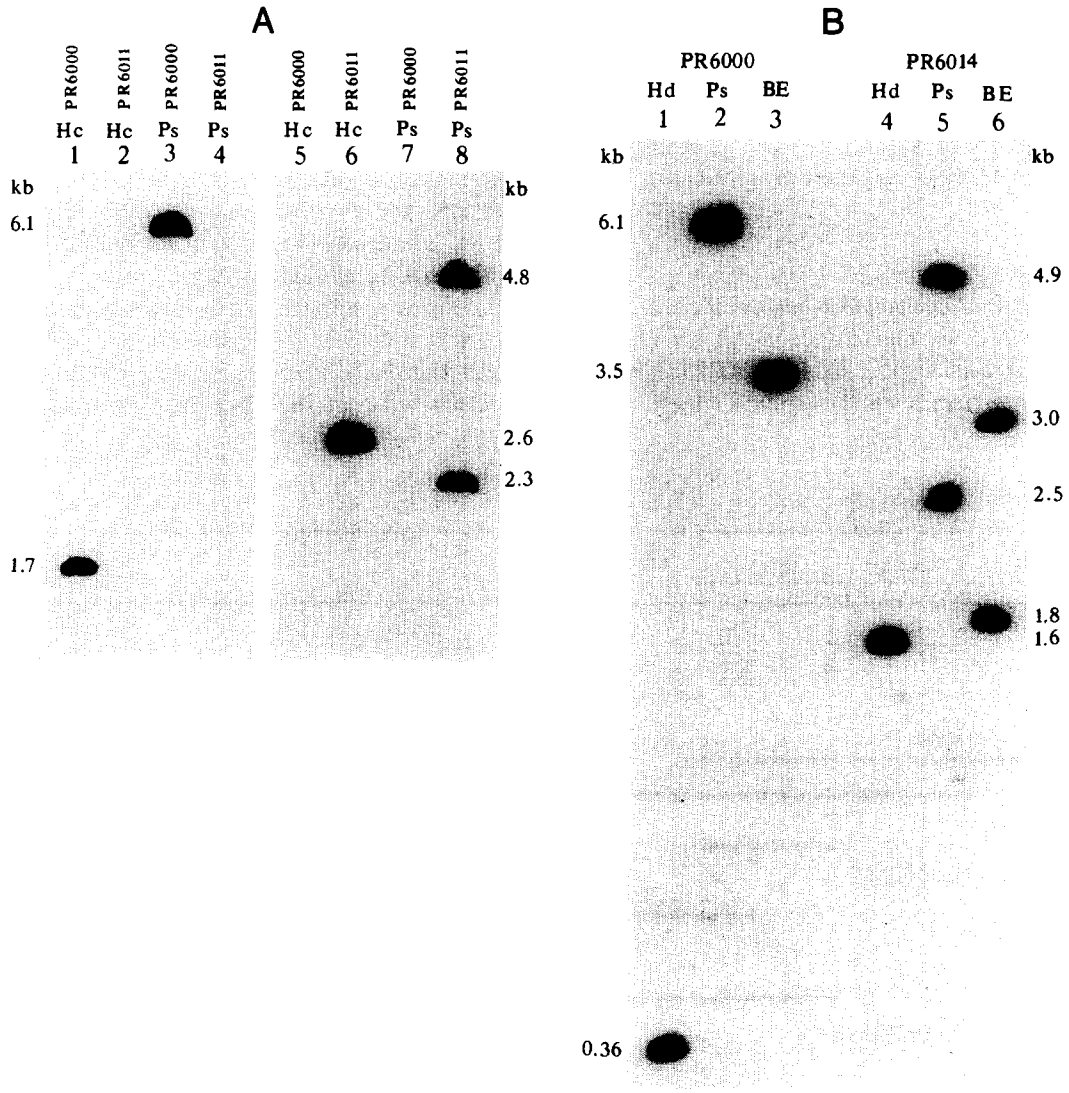

Fig. 3. Southern blot analysis of the *cpcD* locus in strains PR6000, PR6011 and PR6014. (A) PR6000 and PR6011 DNA was digested with *Hin*cII (Hc) or *Pst*I (Ps) and probed with the 358 bp *Hin*dIII fragment containing *cpcD* (lanes 1–4) or a 1.3 kb *Hin*dIII/*Sma*I fragment containing the *aph* gene (Km^r) of Tn5 (lanes 5–8). (B). PR6000 and PR6014 DNA was digested with *Hin*dIII (Hd), *Pst*I (Ps) or *Bgl*II plus *Eco*RI (BE) and probed with the 358 bp *Hin*dIII fragment containing *cpcD*. Sizes of hybridizing species, in kilobase pairs, are shown.

Subsequently, the amino-acid sequence of an 8.9 kDa rod-associated linker from *Fischerella* sp. PCC 7603 was reported [14] which bore considerable homology to the product of the open reading frame. These correlations, combined with the genetic evidence presented below, led us to conclude that the open reading frame in question is a gene, designated *cpcD*, which encodes LR9. Southern blotting and genetic experiments show that *cpcD* is a single copy gene.

Mutation of cpcD

Mutating this gene would test the hypothesis that it encoded LR9 and, if the hypothesis was supported, might also reveal the function of this polypeptide. We employed essentially the same strategy for mutating *cpcD* as for *cpcBA* and *cpcC* [4,15], i.e., deletion or interruption in vitro of the targeted gene by a selectable marker, followed by transformation of the mutated clone into the wild-type strain. Selection for the marker in transformants leads to co-selection of the mutated target gene.

The first mutation of *cpcD* constructed was a deletion of the 358 bp *Hin*dIII fragment, removing the entire coding region as well as 83 bp on its 5′ side and 28 bp on the 3′ side. Replacing the *Hin*dIII fragment was a 1.3 kb *Hin*dIII/*Sma*I fragment of transposon Tn5 which carries the structural gene for aminoglycoside 3′-phosphotransferase II (Materials and Methods). The structure of the resulting clone, called pAQPR56, is shown in Fig. 1, and the bounds of deleted nucleotide sequence are indicated in Fig. 2. Note that the *aph* (Km^r) gene is oriented with the same polarity as *cpcBAC*.

pAQPR56 was transformed into wild type *Synechococcus* sp. PCC 7002, which we refer to herein as strain PR6000. One purified transformant, designated PR6011, was chosen for analysis. Southern blotting proved that PR6011 contained a *cpcD* locus mutated according to the structure of pAQPR56. Fig. 3A displays Southern blots of genomic DNA from PR6000 and PR6011 digested with either *Pst*I or *Hin*cII. When probed with the *cpcD*-containing 358 bp *Hin*dIII fragment from pAQPR50, PR6000 shows homology to a 6.1 kb *Pst*I fragment and a 1.7 kb *Hin*cII fragment, as expected from the structure of pAQPR50 (Fig. 1). On the other hand, PR6011 DNA has no probe-homologous fragment in either digest. When probed with the *aph*-encoding 1.3 kb *Hin*dIII/*Sma*I fragment, PR6000 DNA shows no homology, as expected. PR6011 DNA, however, has two homologous *Pst*I fragments, 2.3 and 4.8 kb, and a single homologous *Hin*cII fragment of 2.6 kb. The sizes of these restriction fragments are compatible with the location and orientation of the *aph* fragment in pAQPR56. Thus *cpcD* is deleted in PR6011. This particular allele is called *cpcD*1.

For reasons described below, we generated a second mutation of *cpcD* which directly affected the coding region only, sparing its flanking sequences. To this end, the clone pAQPR56-2, shown in Fig. 1, was constructed. This clone has a deletion that is limited to 65 bp within *cpcD*, but contains the same marker fragment as pAQPR56. In Fig. 2 the bounds of nucleotide sequence deleted in pAQPR56-2 are indicated. This clone was transformed into PR6000, generating strain PR6014.

Southern blots of PR6000 and PR6014 genomic DNA were probed with the 358 bp *Hin*dIII fragment containing *cpcD*. Blotted DNAs had been digested with either *Hin*dIII or *Pst*I, or a combination of *Bgl*II plus *Eco*RI (Fig. 3B). Each digest of wild-type DNA has a single fragment homologous to the probe: either 0.36 kb (*Hin*dIII), 6.1 kb (*Pst*I), or 3.5 kb (*Bgl*II + *Eco*RI). DNA from PR6014 has a single probe-homologous *Hin*dIII fragment (1.6 kb), two homologous *Pst*I fragments (2.5 and 4.9 kb), and two fragments (1.8 and 3.0 kb) in the *Bgl*II/*Eco*RI digest. The sizes of probe-homologous fragments in all three digests of PR6014 DNA match those expected from the structure of pAQPR56-2. No restriction fragments characteristic of the wild-type *cpcD* locus were detected in PR6014 genomic DNA.

Characterization of PR6011

Cultures of this strain grew with a doubling time that was 1.4-times greater than wild-type under 240 $\mu E/m^2$ per s of photosynthetically active radiation, and 1.7-times greater in 110 $\mu E/m^2$ per s [2]. Absorption spectra of whole cells showed that in PR6011 the ratio of phycobiliproteins to chlorophyll proteins was not noticeably different from PR6000 (data not shown). Spectra of membrane-free cell extracts were also identical for the two strains, demonstrating that the ratio of PC to AP did not differ between them (data not shown). Fluorescence emission spectra of whole cells were recorded with 550 nm excitation, absorbed primarily by phycobiliproteins and less so by chlorophyll proteins (Fig. 4A). PR6000 shows maximal emission at 656 nm, due to phycobiliproteins, and an inflection at 685 nm due to emission by chlorophyll proteins. PR6011 cells show a phycobiliprotein emission shifted to shorter wavelengths, with a maximum at 649 nm. This is indicative of increased fluorescence from PC, and not from components of the phycobilisome core.

Phycobilisomes were purified from PR6000 and PR6011 cultured simultaneously under identical conditions of temperature, light intensity, gas exhange and culture mixing (Materials and Methods). The soluble fraction of cell lysates was centrifuged through a sucrose concentration gradient, from which phycobilisomes were removed in essentially pure form. In sucrose gradients of wild-type cell extracts most of the phycobiliprotein sediments as a homogeneous band, with less than 3% sedimenting as a slower zone. This slow zone consists of

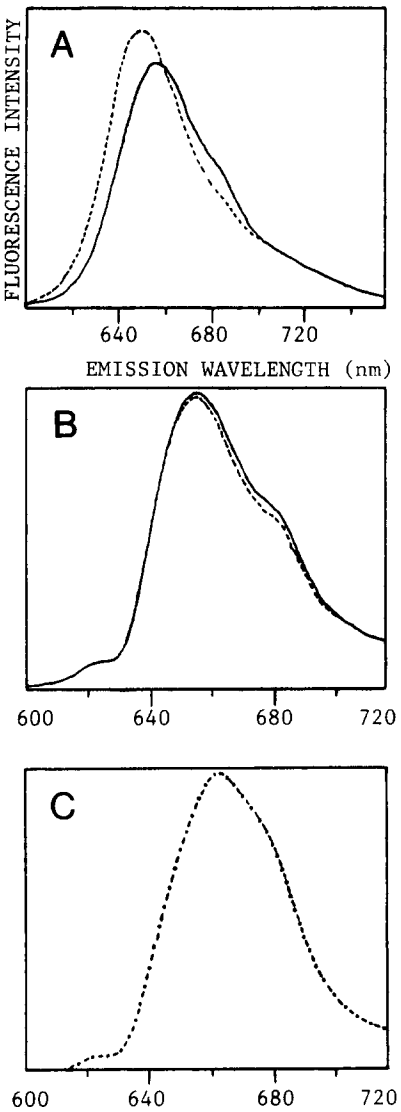

Fig. 4. Uncorrected fluorescence emission of intact cells and purified phycobilisomes. Spectra are of samples matched to identical absorbance at the excitation wavelength. (A) Cells of PR6000 (solid line) and PR6011 (dashed line) excited at 550 nm. (B) Cells of PR6000 (solid line) and PR6014 (dashed line) excited at 550 nm. (C) Phycobilisomes of PR6000 (dashed line, F_{max} 663 nm) and PR6014 (dotted line, F_{max} 662 nm), excited at 580 nm.

AP and PC in approximately equal proportion. Sucrose gradients of PR6011 extracts contained a much larger fraction of phycobiliprotein in the slow zone, approx. 25%. Furthermore, its phycobilisome zone sedimented noticeably slower than did the wild-type zone.

In Fig. 5A is displayed the absorption spectra of phycobilisomes from PR6000, PR6011 and PR6009. The latter strain, which is mutated in *cpcC*, possesses phycobilisomes with half the wild-type level of PC [4]. The spectra have been normalized at 660 nm, where absorption is due almost exclusively to AP and other components of the core domain. Therefore the intermediate absorbance by PR6011 phycobilisomes reflects a PC content approx. 70% that of PR6000. The difference spectrum, i.e., wild-type minus PR6011 (Fig. 5B), is very similar to that of the PC-LR33 complex, with a maximum absorbance at 629 nm [4]. Hence, PR6011 phycobilisomes appear to lack a fraction of PC which in the wild-type is attached to the ends of rods by LR33. The absorption spectrum of the slowly sedimenting phycobiliprotein fraction from PR6011 is shown in Fig. 5B. It is shifted to shorter wavelengths compared to the PC-LR33 complex, absorbing maximally at 625 nm, and thus appears to be almost entirely linker-free PC. The slightly greater absorbance of this fraction at wavelengths above 650 nm is due to contaminating membrane material. We have calculated that approx. 30% of total PC is represented in the slowly sedimenting zone.

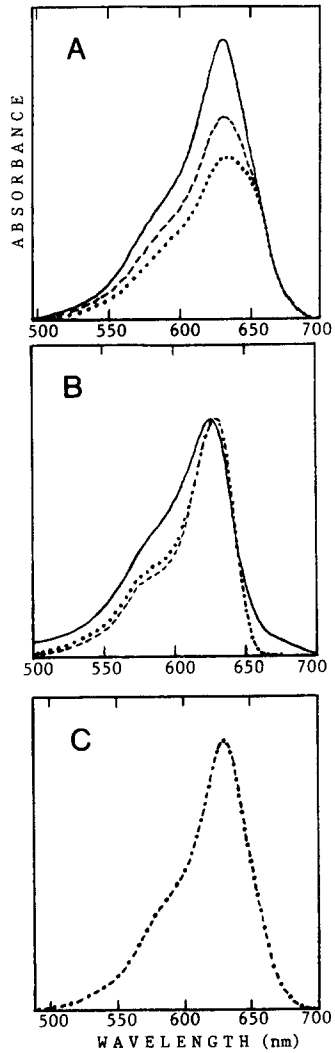

Fig. 5. Absorption of phycobiliprotein fractions from sucrose gradients. (A) Phycobilisomes of PR6000 (solid line, A_{max} 630 nm), PR6011 (dashed line, A_{max} 631 nm) and PR6009 (dotted line, A_{max} 633 nm). (B) Slowly sedimenting fraction of PR6011 (solid line, A_{max} 625 nm), difference of PR6000 minus PR6011 (dashed line, A_{max} 629 nm), and difference of PR6000 minus PR6009 (dotted line, A_{max}629 nm). (C) Phycobilisomes of PR6000 (dashed line, A_{max} 630 nm) and PR6014 (dotted line, A_{max} 630 nm). All spectra are normalized at the wavelength of maximum absorption.

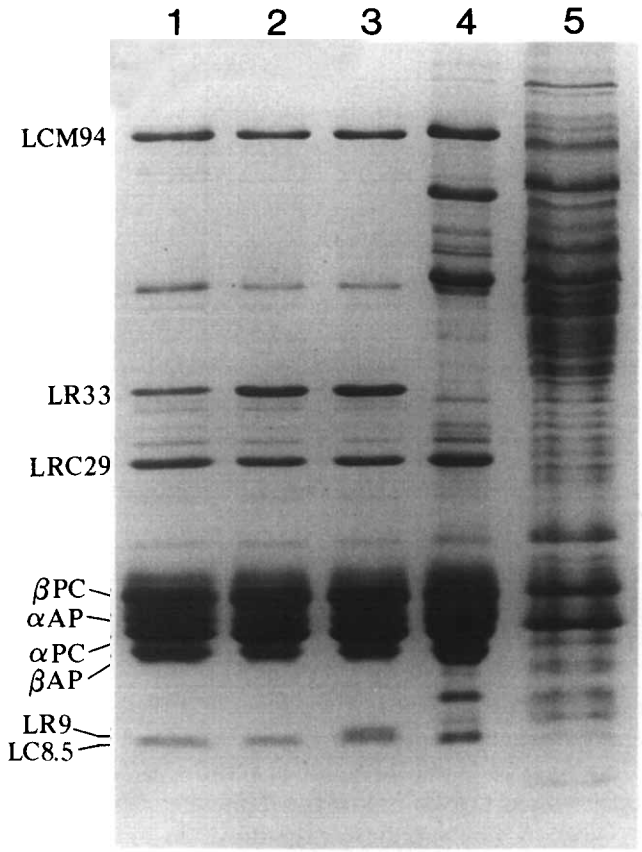

Fig. 6. Gel electrophoresis of phycobiliprotein fractions from sucrose gradients. Lane 1, phycobilisomes from PR6011; lane 2, phycobilisomes from PR6014; lane 3, phycobilisomes from PR6000; lane 4, phycobilisomes from PR6009; lane 5, slowly sedimenting phycobiliprotein fraction from PR6011. The identities of linker polypeptides and phycobiliproteins are labeled on the left. Not indicated are the β18 subunit, which co-migrates with αAP, and the αAPB subunit, which co-migrates with αPC.

Thus the ratio of total PC to AP is the same in both strains, but about 30% of the PC in PR6011 is unattached to phycobilisomes. Since cells of this strain display higher PC fluorescence (Fig. 4A), we believe that the unattached fraction found in vitro is also energetically uncoupled in vivo.

Polypeptide components of phycobiliprotein zones from sucrose gradients were fractionated by electrophoresis in polyacrylamide gels (Fig. 6). Purified phycobilisomes from the two strains contain the same set of polypeptides, except for the absence of detectable LR9 in PR6011 (Fig. 6, lanes 1 and 3). For comparison, phycobilisomes of the *cpcC*$^-$ mutant, which has been shown to lack LR33 and LR9 [4], are also shown. Thus, the single species in PR6011 which has a mobility similar to LR9 is the AP-associated linker LC8.5. Hence mutation of *cpcD* is correlated with the loss of LR9. In addition to this difference, phycobilisomes of PR6011 reproducibly contain less LR33 than the wild-type. Quantitation of linkers by scanning densitometry of stained gels shows that the ratio of LCM94 to LRC29 is identical in both strains, but the ratio of LR33 to LRC29 in PR6011 is 35–40% of the wild-type value. The staining intensity of PC subunits with respect to AP is also noticeably lower in PR6011. In the wild-type, approximately half the PC is linked to phycobilisomes by LR33. If PR6011 has 35–40% of the wild-type amount of this linker, then its phycobilisomes are expected to have about 70% the wild-type level of PC. This matches the deficiency calculated from the absorbance of PR6011 phycobilisomes.

Gel electrophoresis of the slowly sedimenting phycobiliprotein fraction from PR6011 (Fig. 6, lane 5) shows that it is a complex mixture of polypeptides. The α and β subunits of PC are prominent and AP subunits, if present, constitute a minor fraction of phycobiliprotein, perhaps less than 5%. It is also apparent that the PC-associated linker polypeptides LR33 and LRC29 are absent or very minor constituents of this fraction. In particular, the 60–65% deficiency of LR33 in PR6011 phycobilisomes cannot be accounted for if it is bound to PC of the slow fraction.

The foregoing findings lead to two hypotheses. The first is that the *cpcD1* mutation primarily affects only LR9, the loss of which causes secondary phenotypes such as the reduced level of LR33 and the occurrence of uncoupled PC. The second hypothesis is that the *cpcD1* mutation affects the expression of LR9 and LR33 independently. The former linker is lost because its gene is deleted; the second is decreased because sequences controlling its expression are affected (see Discussion). The most direct approach to distinguish between these two schemes was to construct a mutation of *cpcD* in which only the structural gene was affected, and not flanking sequences. For this reason strain PR6014 was produced.

Characterization of PR6014

Unlike PR6011, cultures of this strain grew at a rate that was not measurably different from the wild-type under photosynthetically active radiation of 50 or 200 $\mu E/m^2$ per s. They also had the same pigment composition as wild-type, demonstrated by their identical absorption spectra (not shown). Unlike PR6011, strain PR6014 did not display enhanced fluorescence of phycobiliproteins, with maximal emission at 655 nm (Fig. 4B). Also, sucrose gradients of phycobilisome preparations from strain PR6000 and PR6014 had identical distributions of phycobiliprotein. In both cases the phycobilisome zones sedimented at the same rate, and less than 3% of the phycobiliproteins were in a slowly sedimenting band.

The absorption spectra of PR6014 and PR6000 phycobilisomes do not detectably differ (Fig. 5C), nor do their fluorescence emission spectra (Fig. 4C). Neither is there any difference between the two strains in terms of the polypeptide composition of their phycobilisomes, except that LR9 is absent in PR6014 (Fig. 6 lane 2).

Like PR6011, this strain contains LC8.5 as the sole polypeptide of this mass range. Further evidence that the missing polypeptide in PR6014 and PR6011 is not LC8.5 stems from the fact that their phycobilisomes do not resemble those of a mutant which lacks only this linker [16]. Unlike PR6011, phycobilisomes of PR6014 do not differ from the wild-type in the ratio of LR33 to LRC29.

In the analysis presented thus far, the sole phenotype of the *cpcD2* mutation is an absence of LR9 in phycobilisomes. Therefore, the additional characteristics observed in the *cpcD1* mutant, i.e., decreased LR33 and uncoupled PC, are not dependent on mutation of the structural gene for LR9. Most likely they arise from deletion of intercistronic sequences by the *cpcD1* mutation (Discussion).

Since the loss of LR9 from phycobilisomes had no obvious consequences for function, as determined by absorbance and fluorescence, we explored the possibility of altered phycobilisome structure. As mentioned previously, phycobilisomes from PR6014 sedimented as did the wild-type. However, the relevant zone in sucrose gradients of the mutant did appear to be slightly broader, suggesting a more heterogeneous population of phycobilisomes. To allow a more detailed assessment of structure we performed electron microscopy of isolated phycobilisomes.

Electron microscopy

Phycobilisomes were prepared from cultures of PR6000 and PR6014 grown simultaneously under identical conditions. Within 1 h of isolation the phycobilisomes were mounted and negatively stained for electron microscopy. Micrographs of phycobilisomes from both strains are shown in Fig. 7A and B. Most particles show the structure typical of hemidiscoidal phycobilisomes in face view [17]. In each there is a core region surrounded by five or six (less commonly four) rods. The latter are comprised of from one to five discs, each being a complex of one linker molecule and a hexamer of PC subunits, $(\alpha PC\beta PC)_6$. Discs adjacent to the core contain LRC29 as the only linker [4,13]. It binds the disc, and the entire rod, to the core. In vitro assembly experiments in *Synechococcus* sp. PCC 6301 suggest that discs containing this linker are not found at positions other than the core-proximal terminus of rods [19,20]. Hence it is believed that all discs adjacent to the core contain LRC29; subsequent discs, if present, contain other linkers [20,21]. In the case of PR6000 these can be LR33 and LR9, while in PR6014 the only other rod linker is LR33.

Having adopted the foregoing model of phycobilisome organization, we analyzed micrographs of PR6000 and PR6014 phycobilisomes. In terms of overall organization and substructure we found no obvious differences in the two strains (Fig. 7A and B). To permit a more detailed comparison we evaluated three parameters: the number of rods per phycobilisome, the number of discs per rod, and the number of discs per phycobilisome. Values for the first two parameters are presented in Table IA and B. Data for the third are shown in the histogram of Fig. 8A. For each strain the measurements were obtained from a sample of 108 phycobilisomes.

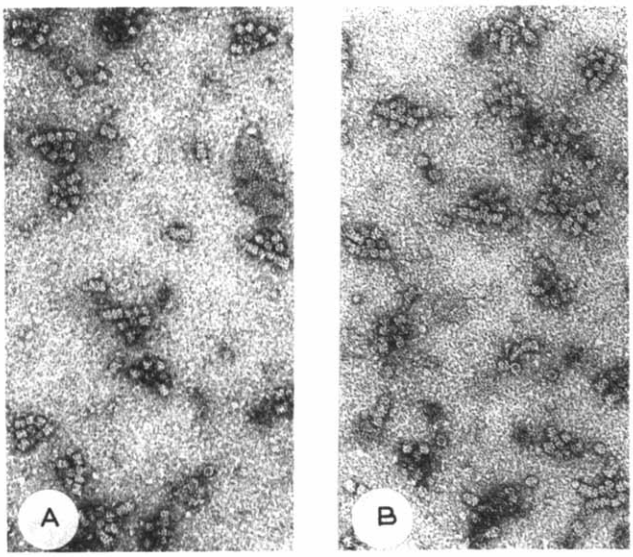

Fig. 7. Electron micrographs of phycobilisomes. (A) From the wild-type strain, PR6000. (B) From the *cpcD2* strain PR6014. Both are shown at a magnification of 108 000×.

(1) Number of rods per phycobilisome. The mean number of rods per phycobilisome was 5.56 for PR6000 and 5.47 for PR6014. The difference between the two means is not significant ($P > 0.1$). The proportion of phycobilisomes having four, five or six rods was also tested and found not to be significantly different between the two strains ($P > 0.1$). Particles which could be con-

TABLE I

Parameters of phycobilisome structure in PR6000 and PR6014, evaluated by electron microscopy

(A) Rods per phycobilisome

Strain	Number of PBS [a] with n rods			Total PBS	Mean rods/PBS
	$n=4$	$n=5$	$n=6$		
PR6000	4	40	64	108	5.56
PR6014	11	35	62	108	5.47

(B) Discs per rod

Strain	number of rods with n discs						Total rods	Mean discs/rod
	$n=1$	$n=2$	$n=3$	$n=4$	$n=5$	$n>5$		
PR6000	52	455	79	10	4	0	600	2.10
PR6014	128	340	88	21	10	4 [b]	591	2.08

[a] PBS: phycobilisome.

[b] 3 rods with 6 discs, 1 rod with 7.

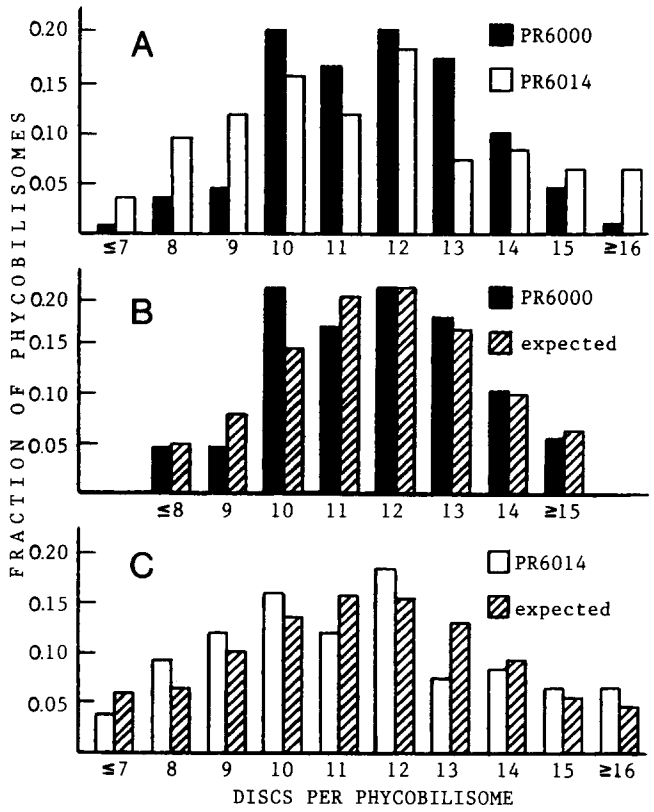

Fig. 8. Frequency distributions of the number of discs per phycobilisome, determined by electron microscopy. (A) Data from PR6000 (solid bars) and PR6014 (open bars). (B) Data from PR6000 (solid bars) compared to the distribution expected from a model of random assortment of rods on phycobilisome cores (hatched bars). (C) Data from PR6014 (open bars) compared to the distribution expected from the model (hatched bars).

strued as phycobilisomes with fewer than four rods were very rare and excluded from both samples. Finding no significant difference between the strains in terms of rods per phycobilisome agrees with data from scanning densitometry of gel-resolved phycobilisome polypeptides (see above). In that case we found no difference between the strains in their ratio of LRC29 to LCM94. Since LRC29 connects a rod to the core any change in the number of rods per phycobilisome ought to be accompanied by a similar change in the ratio of LRC29 to core components.

(2) Number of discs per rod. The mean number of discs per rod ($\pm$variance) was 2.10($\pm$0.34) for wild-type and 2.08($\pm$0.78) for *cpcD2* phycobilisomes. These two means do not differ significantly ($P > 0.1$). However, the proportions of rods having, 1, 2,... $\geqslant 5$ discs were significantly different in the two strains ($P < 0.01$). From the data in Table IB it is apparent that wild-type phycobilisomes have a narrower range of rod-lengths than the *cpcD2* strain. This is reflected in a significantly greater variance in the mean number of discs/rod for the mutant strain ($P < 0.01$).

Finding the same mean rod length in the two strains is in agreement with data presented above. In the model of rod organization outlined previously, LRC29 is placed at the core-proximal disc only, with each subsequent disc containing one molecule of LR33. Thus, in a population of phycobilisomes the ratio of LR33 to LRC29 is directly related to average rod length. The ratio of these two linkers was quantitated by scanning densitometry (see above) and found to be the same for PR6000 and PR6014, agreeing with the rod length data.

The results outlined thus far show that in strain PR6014, the rod linker polypeptides, LRC29 and LR33, are functional and present at wild-type levels in phycobilisomes. However, there is a greater variability of rod-length in this mutant. In an attempt to describe factors which might contribute to variation in the number of discs per rod we considered the types of inter-disc association which occur.

There are two classes of disc-to-disc connections, one between an LRC29-containing disc (denoted an A disc) and an LR33-containing disc (denoted as a B disc), and one between two LR33-containing discs; i.e., A-B connections and B-B connections, respectively. The degree to which A-B connections are preferred over the B-B type will determine uniformity of rod length. For example, supposing the number of A and B discs to be equal, then if A-B connections are highly preferred over the B-B type all rods will be uniform, consisting of one A disc and a single B disc. If B-B associations are preferred then most rods will consist of an A disc only, while a few will be extremely long, composed of numerous tandem B discs attached to a single core-proximal A disc. One indication of relative preference is the ratio of A-B to B-B connections, A-B/B-B. To compare phycobilisome populations in terms of this ratio it is essential that they have the same relative number of A and B discs. This is largely true for those analyzed here, where the ratio A/B is 0.91 for PR6000 and 0.92 for PR6014. From the data in Table I for wild-type rods we counted 548 A-B and 111 B-B connections, giving an A-B/B-B ratio of 4.94. For *cpcD2* the ratio is 2.62 (A-B/B-B = 463/178). By this criterion, then, the preference of A-B associations is higher in wild-type than PR6014 by a factor of 4.94/2.62, or 1.9. Thus, the presence of LR9 is correlated with a nearly 2-fold increase in the frequency with which A and B discs mutually associate.

(3) Number of discs per phycobilisome. Distributions of discs/phycobilisome in wild-type and *cpcD2* strains are displayed in Fig. 8A. The mean ($\pm$variance) of discs per phycobilisome is 11.66 ($\pm$3.38) for wild-type and 11.40 ($\pm$7.24) for *cpcD2*. The means are not significantly different ($P > 0.1$); however, the variance in discs per phycobilisome is significantly greater in the *cpcD2* strain ($P < 0.01$). In other words, phycobilisomes from PR6014 are more heterogeneous in size. Spectrophoto-

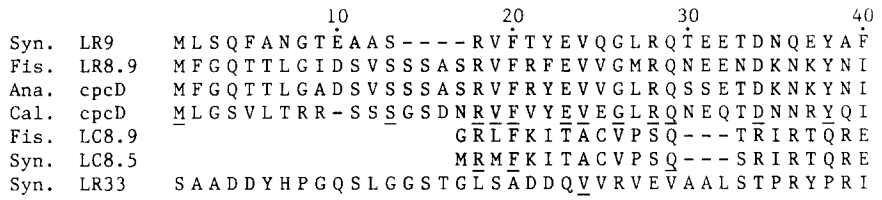

Fig. 9. Amino-acid sequences of linker polypeptides. Sources are as follows. Syn. LR9: *Synechococcus* sp. PCC 7002, PC-associated linker encoded by *cpcD* (present work). Fis. LR8.9: *Fischerella* sp. PCC 7603, PEC-associated linker determined by amino-acid sequence analysis [14]. Ana. *cpcD*: *Anabaena* sp. PCC 7120, open reading frame located 3′ to another which may encode LR32 [26]. Cal. *cpcD*: *Calothrix* sp. PCC 7601, open reading frame (*lpcC*) located 3′ to *lpcB*, which encodes LR39 [25]. Fis. LC8.9: *Fischerella* sp. 7603, AP-associated linker, determined by amino-acid sequence analysis [23]. Syn. LC8.5: *Synechococcus* sp. PCC 7002 AP-associated linker encoded by *apcC* [2]. Syn. LR33: *Synechococcus* sp. PCC

metric data presented above demonstrated that the ratio of PC to AP was identical in phycobilisomes of the two strains, in agreement with finding the same mean number of discs per phycobilisome. We believe that the slightly broader phycobilisome zone found in sucrose gradients of PR6014 is a manifestation of greater variation in size.

Results for this parameter are reminiscent of the disc/rod parameter in that no difference was found between the means, but the variance was significantly higher in *cpcD2*. We were thus led to consider whether, for a given strain, variation in rod length determines variation in discs/phycobilisome. That is, suppose the six rods which occur on a phycobilisome have lengths which are independent of each other. Then the distribution of the total number of discs per phycobilisome is expected to be normal. The mean number of discs per phycobilisome will be 6-times the mean rod length, and the variance in discs per phycobilisome will be 6-times the variance of rod length [22]. Knowing the mean and variance of rod length for the two strains, we applied the normal distribution to calculate the expected distribution of discs/phycobilisome, as shown in Fig. 8B and C. Note that we have assumed exactly six rods per phycobilisome when there are actually about 5.5. This inconsistency was overcome by taking the absence of a rod to be equivalent to a rod with zero discs. The mean and variance of discs/rod was then recalculated for the two samples of phycobilisomes. The values obtained, mean ($\pm$variance), were 1.94 ($\pm$0.61) for wild-type rods, and 1.90 ($\pm$1.06) for *cpcD2*. As before, the mean rod lengths do not differ significantly, but the variance for *cpcD2* rods is significantly greater than for wild-type rods.

For each sample the expected distribution of discs/phycobilisome was tested for goodness-of-fit to the data and found to be acceptable ($P > 0.3$ for PR6000, $P > 0.3$ for PR6014). Hence, variation in the number of discs per phycobilisome is consistent with the hypothesis that rods occur on phycobilisomes independently of their individual lengths. A corollary is that there appears to be no mechanism in the assembly of phycobilisomes that compensates for the inherent heterogeneity of rod lengths in order to generate phycobilisomes having a fixed number of discs. In this sense LR9 indirectly limits the range of phycobilisome mass by restricting variation in rod length.

Discussion

Amino-acid sequence homology among linkers

All phycobilisomes yet charaterized contain linkers of low apparent mass, about 7–10 kDa. Amino-acid sequences are known for three small linkers which have been directly identified. These are LC8.9 and LR8.9 from *Fischerella* sp. PCC 7603 [14,23] and LR9 from *Synechococcus* sp. PCC 7002 (present work). Data from the first two linkers were obtained by sequencing the isolated polypeptides; a sequence for the third was determined by deduction from the nucleotide sequence of its gene. Each of these linkers is associated with a different class of phycobiliprotein. LC8.9 and LR8.9 from *Fischerella* sp. were isolated as complexes with AP and phycoerythrocyanin (PEC) respectively. LR9 from *Synechococcus* sp. PCC 7002 is associated with PC (Ref. 4, present work). A comparison of these sequences is shown in Fig. 9.

The two small rod linkers show more homology to each other (55% of residues are conserved) than each has with the AP-associated linker (approx. 21%). This is correlated with the relationships among their respective phycobiliproteins. That is, PC and PEC share more homology (about 65%) than either shares with AP (about 30%) [24]. Sequence homology among the small linkers is largely clustered in two segments of the polypeptides, one from residues 18 to 29 (as numbered in Fig. 9), and another region from residues 50 to 72. This latter segment is in fact homologous to a region near the carboxyl termini of larger rod linkers which have been directly identified; LR33 from *Synechococcus* sp. PCC 7002 [4] (shown in Fig. 9), LR34.5PEC from *Fischerella* sp. [14], and LR39 from *Calothrix* sp. PCC 7601 [25].

From *Calothrix* sp. and *Anabaena* sp. PCC 7120 have been cloned genes which probably encode the small rod-linkers of these organisms [25,26]. The identities of these genes, *lpcC (cpcD)* from the former species and *cpcD* from the latter, have been inferred from two criteria. Firstly, amino-acid sequence homology between

```
          50          60          70          80
RRSGSVFINVPYARMNQEMQRILRLGGKIVSIKPYTGATASDEE*
RRSGSVYITVPYNRMSEEMQRIHRLGGKIVKIEPLTRAAG*
RNSGSVFITVPYSRMNEEYQRITRLGGKIVKIEQLVSAEA*
RNSSTIEIQVPYSRMNEEDRRITRLGGRIVNIRPAGENPTEDASEN*
LQNTYFTKLVPYENWFREQQRIQKMGGKIVKVELATGKQGINTGLA*
LQNTYFTKLVPYDNWFREQQRIMKMGGKIVKVQLATGKPGTNTGLT*
RRSSRVFF-VPVSRLSQKLQEIQRMGGRVASISPAGQ*
```

7002, PC-associated linker encoded by *cpcC* [4]. Only the carboxyl terminal 77 residues of the latter are shown. An underlined residue is found in all the small rod-linkers listed above it. Amino acid residues are abbreviated as follows: A, alanine; C, cysteine; D, apartic acid; E, glutamic acid; F, phenylalanine; G, glycine; H, histidine; I, isoleucine; K, lysine; L, leucine; M, methionine; N, asparagine; P, proline; Q, glutamine; R, arginine; S, serine; T, threonine; V, valine; W, tryptophan; Y, tyrosine.

the putative gene products (Fig. 9) and known small rod linkers is high. Secondly, these genes are located 3′ to the genes for known (*Calothrix* sp.) or putative (*Anabaena* sp.) large rod-linkers. This is analogous to the arrangement in *Synechococcus* sp. PCC 7002, in which the identity of both linker genes is well established (Ref. 2; present work).

Among the four small rod-linkers illustrated in Fig. 9, one pair shows considerably more sequence homology than the others. LR8.9 from *Fischerella* sp. and the *cpcD* product of *Anabaena* sp. have 76% of their residues in common, while other pairs share from 46 to 56% homology. *Anabaena* sp. PCC 7120, like *Fischerella* sp., contains PEC in its phycobilisomes [27], hence its *cpcD* product may be a PEC-associated linker, as is LR8.9 of the latter species. Otherwise, this linker may associate with both PC and PEC.

Location of LR9

There is substantial evidence that LR9 is associated with the terminal PC hexamer of rods. First of all, mutation of *cpcC* leads to loss of both the terminal PC hexamer and LR9 from phycobilisomes [4] (Fig. 6, lane 4). Mutation of *cpcC* probably does not prevent expression of *cpcD*, since two other genes that are 3′ to and co-transcribed with *cpcD* are expressed in the *cpcC*$^-$ strain (Zhou, J.H. and Bryant, D.A., unpublished results). Since LR9 itself does not function in linking PC to form rods, then the absence of LR9 from *cpcC*$^-$ phycobilisomes is a consequence, not a cause, of the uncoupling of the terminal PC hexamer. This observation alone does not rule against the possibility that LR9 is associated with the core-proximal PC hexamer, and is liberated from it when the terminal hexamer is absent. However, other evidence suggests this is not the case. For example, when phycobilisomes are separated into PC and AP fractions by chromatography on hydroxyapatite, three-fourths of the PC co-elutes as a rod complex with LR33 and LRC29. LR9 is associated with the remaining one-fourth of PC [4]. Thus LR9 is not associated with the PC-LRC29 complex even though LR33 is present. A more likely interpretation of this finding is that LR9 is bound to the core-distal trimer of the PC-LR33 complex, and that this trimer is released under the conditions of chromatography. Analogies with other organisms also suggest a terminal location for LR9. For example, the homologous linker of *Fischerella* sp., LR8.9, is bound to PEC, the rod-terminal phycobiliprotein of this organism [28]. Also, red-light-inducible PC in the phycobilisomes of *Pseudanabaena* sp. PCC 7409 contains a small rod linker that is lost, along with this class of PC, when phycoerythrin is synthesized by shifting to green light. However, the core-proximal PC of green-light phycobilisomes is still synthesized [29]. Thus the small linker is associated with PC that is not proximal to the core.

Less direct evidence for the location of LR9 is derived from amino-acid sequence homology among linkers. It is known that approx. 5 kDa at the carboxyl terminus of large rod linkers is proteinase-sensitive and essential for the coupling of adjacent hexamers of PC and/or PEC [21,30]. This portion of the carboxyl end encompasses the region which is most homologous to small rod linkers. According to available evidence, the proteinase-sensitive segment of large rod linkers protrudes from the core-distal face of a hexamer-linker complex and binds to a complementary site at the core-distal face of another such complex, thus joining them [21,30]. On the basis of sequence homology between large and small linkers, the latter are presumed to also have the potential for occupying the site on the core-distal faces of phycobiliprotein-linker complexes. In particular, the hexamer which resides at the core-distal terminus of a rod would have an unoccupied linker-attachment site to which a small linker could bind. In summary, the available evidence is most consistent with a model in which LR9 is bound to the core-distal end of rods.

Function of LR9

Results obtained by mutation of *cpcD* show that LR9 is not required for assembly of intact phycobilisomes. Spectroscopic data on phycobilisomes did not reveal any differences between the mutant and wild-type. However, further observations on isolated subcomplexes of mutant phycobilisomes are needed to detect possible spectroscopic effects of LR9. The only phenotypes attributable to the loss of LR9 are a greater

variance in both the mean number of discs (PC hexamer-linker complexes) per rod and number of discs per phycobilisome. We have shown that the latter phenotype is determined by the former. Thus LR9 appears to function in minimizing the heterogeneity of rod length. From a teleological viewpoint, then, we infer an advantage to rods of uniform length, possibly in regard to the efficiency of energy transfer. Disc-to-disc transfer is the rate-limiting step in the transfer of excitation energy from rods to the core [31]. It is expected that the probability of energy loss due to fluorescence will be higher in a rod composed of several discs than in one with fewer discs. Thus, in considering two populations of phycobilisomes that differ only in their range of rod-lengths, the population with the largest range may have a lower efficiency of energy transfer to the core.

The mechanism by which LR9 minimizes the heterogeneity of rod length is unknown. A simple hypothesis can be proposed which is based on the location of LR9 at a site on the core-distal face of the $(\alpha PC,\beta PC)_6$-LR33 complex. In the absence of LR9 this site is available for binding to another such complex, which in turn may bind yet another. Thus rods containing three or more discs, including the core-proximal PC-LRC29 disc, will be common. Given a fixed ratio of PC-LR33 to PC-LRC29 discs, the fraction of rods comprised of only the latter, i.e., one-disc rods, must also be high. On the other hand, occurrence of LR9 at the core-distal face of a PC-LR33 disc will preclude the tandem joining of such units. As a result, the formation of rods longer or shorter than two discs will be minimized. A manifestation of this would be an apparent increase in the specificity with which PC-LR33 and PC-LRC29 discs associate when LR9 is present. The fact that some rods in wild-type phycobilisomes do contain three or more discs may reflect a stoichiometric deficiency of LR9 or a competition between LR33 and LR9 for binding at the same attachment site.

Depletion of LR33 in PR6011

Finally, we address the observation of a specific decrease in LR33 in the *cpcD1* mutant. This mutation deletes the structural gene of *cpcD* as well as flanking intercistronic sequences. In particular, two prominent inverted repeats between *cpcC* and *cpcD*, as indicated in Fig. 2, are affected. It has been found that the *cpcD* transcript is part of a larger one containing *cpcBAC* as well (Gasparich, G. and Bryant, D.A., unpublished results). In this transcript, inverted repeats are expected to form intrastrand stem-loop structures. The presence of inverted repeats coincides with the 3′ termini of mRNA species in cyanobacteria [32–34]. In *E. coli* and the photosynthetic bacteria it has been demonstrated that stem-loops enhance the lifetime of RNA sequences located to their 5′ side [35,36]. This function, if operative in cyanobacteria, would account for the decrease in LR33 found in strain PR6011. Deletion of intercistronic stem-loops between *cpcC* and *cpcD* is expected to lead to a decrease in the lifetime, and hence the steady-state level, of *cpcC* mRNA. The rate of synthesis of LR33 is expected to decrease in proportion to the altered level of its mRNA. Preliminary observations show that the level of *cpcC* mRNA in PR6011, relative to *cpcBA* RNA, is indeed lower than in the wild-type (Zhou, J.H. and Bryant, D.A., unpublished results).

Acknowledgements

This work was supported by grant No. DMB-8510770 from the National Science Foundation to R. de L. and S.E.S.; and by grants No. GM-31625 from the National Institutes of Health and No. 83-CRCR-1-1336 from the U.S. Department of Agriculture to D.A.B. We thank Gerard Guglielmi of the Institut Pasteur for assistance with electron microscopic characterization of phycobilisomes.

References

1 Stevens, S.E., Jr. and Porter, R.D. (1980) Proc. Natl. Acad. Sci USA 77, 6052–6056.
2 Bryant, D.A. (1988) in Light-Energy Transduction in Photosynthesis: Higher Plant and Bacterial Models (Stevens, S.E., Jr. and Bryant, D.A., eds.), pp. 62–90. American Society of Plant Physiologists, Rockville.
3 De Lorimier, R., Bryant, D.A., Porter, R.D., Liu, W.-Y., Jay, E. and Stevens, S.E., Jr. (1984) Proc. Natl. Acad. Sci. USA 81, 7946–7950.
4 De Lorimier, R., Guglielmi, G., Bryant, D.A. and Stevens, S.E., Jr. (1990) Arch. Microbiol, in press.
5 Bryant, D.A., De Lorimier, R., Guglielmi, G., Stirewalt, V.L., Cantrell, A. and Stevens, S.E., Jr. (1987) in Progress in Photosynthesis Research (Biggens, J., ed.), Vol. IV, pp. 749–755, Martinus Nijhoff, Dordrecht.
6 Vieira, J. and Messing, J. (1982) Gene 19, 259–268.
7 Buzby, J.S., Porter, R.D. and Stevens, S.E., Jr. (1983) J. Bacteriol. 154, 1446–1450.
8 Hanahan, D. and Meselson, M. (1983) Methods Enzymol. 100B, 333–342.
9 Sanger, F., Nicklen, S. and Coulson, A.R. (1977) Proc. Natl. Acad. Sci. USA 74, 5463–5467.
10 Buzby, J.S., Porter, R.D. and Stevens, S.E., Jr. (1985) Science 230, 805–807.
11 Henikoff, S. (1984) Gene 28, 351–359.
12 Stevens, S.E., Jr., Patterson, C.O.P. and Myers, J. (1973) J. Phycol. 9, 427–430.
13 Yamanaka, G., Glazer, A.N. and Williams, R.C. (1980) J. Biol. Chem. 255, 11004–11010.
14 Fuglistaller, P., Suter, F. and Zuber, H. (1985) Biol. Chem. Hoppe-Seyler 366, 993–1001.
15 Bryant, D.A., De Lormier, R., Guglielmi, G. and Stevens, S.E., Jr. (1990) Arch. Microbiol., in press.
16 Maxson, P., Sauer, K., Zhou, J., Bryant, D.A. and Glazer, A.N. (1989) Biochim. Biophys. Acta 977, 40–51.
17 Bryant, D.A., Guglielmi, G., Tandeau de Marsac, N., Castets, A.-M. and Cohen-Bazire, G. (1979) Arch. Microbiol. 123, 113–127.

18 Glazer, A.N. (1985) Annu. Rev. Biophys. Biophys. Chem. 14, 47–77.
19 Lundell, D.J., Williams, R.C. and Glazer, A.N. (1981) J. Biol. Chem. 256, 3580–3592.
20 Yu, M.-H., Glazer, A.N. and Williams, R.C. (1981) J. Biol. Chem. 256, 13130–13136.
21 Yu, M.-H. and Glazer, A.N. (1982) J. Biol. Chem. 257, 3429–3433.
22 Walpole, R.E. and Myers, R.H. (1989) Probability and Statistics for Engineers and Scientists (4th Edn.), p. 103, MacMillan, New York.
23 Fuglistaller, P., Rumbeli, R., Suter, F. and Zuber, H. (1984) Hoppe-Seyler's Z. Physiol. Chem. 365, 1085–1096.
24 Fuglistaller, P., Suter, F. and Zuber, H. (1983) Hoppe-Seyler's Z. Physiol. Chem. 364, 691–712.
25 Lomax, T.L., Conley, P.B., Schilling, J. and Grossman, A.R. (1987) J. Bacteriol. 169, 2675–2684.
26 Belknap, W.R. and Haselkorn, R. (1987) EMBO J. 6, 871–884.
27 Bryant, D.A. (1982) J. Gen. Microbiol. 128, 835–844.
28 Nies, M. and Wehrmeyer, W. (1981) Arch. Microbiol. 129, 374–379.
29 Bryant, D.A. and Cohen-Bazire, G. (1981) Eur. J. Biochem. 119, 415–424.
30 Fuglistaller, P., Suter, F. and Zuber, H. (1986) Biol. Chem. Hoppe Seyler 367, 615–626.
31 Glazer, A.N., Yeh, S.W., Webb, S.P. and Clark, J.H. (1985) Science 227, 419–423.
32 Shinozaki, K. and Sugiura, M. (1985) Mol. Gen. Genet. 200, 27–32.
33 Csiszar, K., Houmard, J., Damerval, T. and Tandeau de Marsac, N. (1987) Gene 60, 29–37.
34 Mazel, D., Houmard, J. and Tandeau de Marsac, N. (1988) Mol. Gen. Genet. 211, 296–304.
35 Newbury, S.F., Smith, N.H. and Higgins, C.F. (1987) Cell 51, 1131–1143.
36 Chen, C.-Y., Beatty, J.T., Cohen, S.N. and Belasco, J.G. (1988) Cell 52, 609–619.